The 2nd year report

Crystal Structures, Molecular Modeling, and Morphology of Poly(1,5-naphthalene-benzobisoxazole) and Poly(2,6-naphthalene-benzobisoxazole)

By Soo-Young Park

2006. 2

Tel +82-53-950-5630; Fax +82-53-950-6623; e-mail psy@knu.ac.kr

Materials were supplied from AFRL

1. **Introduction**
2. **Experimental**
   - **2-1. Materials**
   - **2-2. Polymer Synthesis**
   - **2-3. Fiber Processing**
   - **2-4. General Characterization**
   - **2-5 X-ray Studies**
   - **2-6. Molecular Modeling**
   - **2-7. Refinement**
3. **Results and Discussion**
   - **3-1. Polymer synthesis and characterization**
   - **3-2. X-ray patterns**
   - **3-3 Chain Conformation**
   - **3-4. The crystal structure**
     - **3-4-1. Naph-2,6-PBO**
     - **3-4-2. Naph-1,5-PBO**
4. **Conclusions**
5. **References**
6. **PI's *Curriculum Vitae***
7. **Publications**

Report Documentation Page

Form Approved
OMB No. 0704-0188

1. REPORT DATE	2. REPORT TYPE	3. DATES COVERED
27 JUN 2006	**Final Report (Technical)**	**20-08-2004 to 19-09-2005**

4. TITLE AND SUBTITLE
Crystal Structures, Molecular Modeling, and Morphology of Poly(1,5-naphthalene-benzobisoxazole) and Poly(2,6-naphthalene-benzobisoxazole)

5a. CONTRACT NUMBER
FA520904P0505

5b. GRANT NUMBER

5c. PROGRAM ELEMENT NUMBER

6. AUTHOR(S)
Park Soo-Young

5d. PROJECT NUMBER

5e. TASK NUMBER

5f. WORK UNIT NUMBER

7. PERFORMING ORGANIZATION NAME(S) AND ADDRESS(ES)
Kyungpook National University,#1370 Sangyuk-Dong, Buk-gu,Daegu 702-701,NA,Korea

8. PERFORMING ORGANIZATION REPORT NUMBER
AOARD-044006

9. SPONSORING/MONITORING AGENCY NAME(S) AND ADDRESS(ES)
The US Resarch Labolatory, AOARD/AFOSR, Unit 45002, APO, AP, 96337-5002

10. SPONSOR/MONITOR'S ACRONYM(S)
AOARD/AFOSR

11. SPONSOR/MONITOR'S REPORT NUMBER(S)
AOARD-044006

12. DISTRIBUTION/AVAILABILITY STATEMENT
Approved for public release; distribution unlimited

13. SUPPLEMENTARY NOTES

14. ABSTRACT
In this study, the structures of poly(2,6-Naphthalenebenzobisoxazole) (Naph-2,6-PBO) and poly(1,5-Naphthalenebenzobisoxazole) (Naph-1,5-PBO) were delineated using X-ray and molecular modeling methods.

15. SUBJECT TERMS

16. SECURITY CLASSIFICATION OF:			17. LIMITATION OF ABSTRACT	18. NUMBER OF PAGES	19a. NAME OF RESPONSIBLE PERSON
a. REPORT	b. ABSTRACT	c. THIS PAGE			
unclassified	**unclassified**	**unclassified**		**30**	

1. Introduction

Rigid-rod polymers such as poly(*p*-phenylenebenzobisthiazole) (PBT) and poly(*p*-phenylenebenzobisoxazole) (PBO) have attracted attention because of their excellent thermal and thermoxidative stabilities as well as their exceptional tensile strength and tensile modulus, attributable to their inherent chain stiffness and a high degree of molecular orientation, achieved by fiber-spinning from a liquid crystalline solution.[1-16] PBO and PBT fibers have been considered as alternatives to reinforcement aramid and carbon fibers. The crystal structure of PBO has been investigated by several groups.[17-20] One of the prominent characteristics is the axial disorder in the crystal, which causes streaks along the layer lines in the X-ray fiber pattern. The chains in the crystal, however, are not completely random along the chain axis but have a certain registry of adjacent chains, which cause some Laue spots in the X-ray fiber pattern. Fratini *et al.*[17] first reported the crystal structure of PBO in which two molecular chains pass through a metrically monoclinic unit cell with parameters of a=11.20 Å, b=3.54 Å, c=12.05 Å, and g=101.3°, with the plane group of p2; the plane group rather than the space group can be defined as being due to the axial disorder. They adopted non-primitive cells in order to include longitudinal and lateral disorders because primitive cells require perfect registry of adjacent chains and close intermolecular contact occurs between neighboring molecules along the a axis. Thereafter, Martin and Thomas[18] proposed a new structure where the two chains are packed in the same monoclinic unit cell proposed by Fratini *et al.*[17] and the neighboring chains are randomly shifted by between +c/4 and –c/4 along the chain axis in the crystal structure. The occurrence of Laue spots in the X-ray fiber pattern was attributed to this discrete random axial shift in the crystal. Recently, Tashiro *et al.*[19] reported the computer simulation of the fiber pattern of PBO with a more realistic superlattice, where the chains are assumed to form the layers extending along the *110* plane with the relative heights of the adjacent chains in the sheets almost confined to either +c/4 or –c/4 and these sheets are stacked together in the b-axis direction with random heights along the chain axis. Based on the neutron diffraction method, Takahashi[20] reported the crystal structure of PBO where one chain is in the unit cell with parameters of a=5.651Å, b=3.57Å, fiber repeat unit = 12.05 Å (fiber repeat unit instead of c dimension was reported because of the random structure and plane group) and ?=101.4° and the molecular heights of PBO are disordered by c/2. The conformation of PBO is known to be dominated by conjugative effects favoring coplanarity because there is no steric congestion between the benzobisoxazole and phenyl rings. Fratini *et al.*[17] reported the torsion angle between the benzobisoxazole and phenyl ring to be 12° but Takahashi[20] reported a torsion angle of 25.7° from the neutron diffraction study. However, the energy calculation shows that the planar structure (torsion angle = 0°) is stable which is consistent with that observed for low molecular model compounds of PBO as determined by the X-ray structural analysis and which was adopted by Tashiro *et al.*[19]

In this study, the structures of poly(2,6-Naphthalenebenzobisoxazole) (Naph-2,6-PBO) and poly(1,5-Naphthalenebenzobisoxazole) (Naph-1,5-PBO) were delineated using X-ray and molecular modeling methods. Lower geometrical symmetry and extended planar packing of the naphthalene-2,6-diyl and the naphthalene-1,5-diyl structural links relative to *p*-phenylene unit can affect chain conformation, packing, and crystallinity in analogy to the well-known PEN *versus* PET fibers.[21] The

shapes of the chain in the Naph-2,6-PBO and Naph-1,5-PBO polymers are kinked compared to PBO due to the 2,6- and 1,5- positions at which the naphthalene ring extends. The kinked structures can distinguish the crystal structures of Naph-1,5-PBO and Naph-2,6-PBO from that of PBO in terms of the axial disorder. Additionally, Naph-1,5-PBO has a more kinked chain structure than Naph-2,6-PBO since it is also influenced by steric hindrance due to the proximity of the α-hydrogen of the naphthalene ring and the hetero atoms of the benzoxazole ring. In this study, the effects of kinked structure and steric hindrance between the naphthalene and heterocyclic rings on the disordered structure will be explored using X-ray and molecular modeling methods. The analysis of their crystal structures would be very interesting from the structural point of view since the kinked structure can reduce the axial shift and increase inter-chain interactions.

While this paper mainly focuses on the X-ray analysis of these naphthalene-based polybenzobisoxazole structures and their molecular modeling, details of the synthesis of the polymers and their general characterization are also given. While poly(2,6-Naphthalenebenzobisoxazole) composition is referred to in a Japanese patent[22], properties of this rigid-rod polymer have not been described in the literature. Poly(1,5-Naphthalenebenzobisoxazole), the other aromatic heterocyclic polymer described in this study, is relatively unknown.

2. Experimental

2-1. Materials

4,6-Diaminoresorcinoldihydrochloride was purchased from TCI America. It was further purified by recrystallization from Conc.HCl in the presence of $SnCl_2.2H_2O$. 2,6-Naphthalenedicarboxylic acid was received from TCI America and used without further purification. 1,5-Naphthalenedicarboxylic acid was prepared as described by us previously.[23, 24] It was recrystallized from ethanol prior to use in polymerization.

2-2. Polymer Synthesis

The polycondensation between the naphthalenedicarboxylic acid monomer and 4,6-diaminoresorcinoldihydrochloride in polyphosphoric acid (PPA) using the "P_2O_5 adjustment method"[25] is described below for the two polymers.

Synthesis of Poly(benzobenzobisoxazole) containing naphthalene-2,6-diyl unit (Naph-2,6-PBO)

Into a resin flask fitted with a high torque mechanical stirrer, a nitrogen inlet/outlet adapter and a side opening for addition, was placed 4.32 g (0.02 mole) of 2,6-naphthalenedicarboxylic acid, 4.26 g (0.02 mole) of 4,6-Diaminoresorcinoldihydrochloride and 24.55 g of freshly prepared 77 % PPA. The monomers were stirred in PPA and the resulting mixture was dehydrochlorinated over a period of 24 hours under a nitrogen flow, slowly raising the temperature to 105 °C to avoid foaming. After the degassing was complete, the mixture was cooled and 15.70 g of 99 % P_2O_5 was added to ensure a final polymer concentration of 12 wt % in PPA. The mixture was maintained at 100 °C with stirring to ensure good homogeneity and the temperature was then raised to 165 °C and the polymerization was run

overnight. During this process, stir -opalescence characteristic of the anisotropic phase of the polymer in PPA, was observed. The polycondensation was continued at 180 °C for four hours and ~ 40 g of the viscous polymer dope was taken out for the fiber spinning process. The remaining dope was placed in large quantities of distilled water and the fibrous polymer was chopped up in a Waring blender. The polymer was filtered off, soxhlet-extracted with hot water and finally dried *in vacuo* at 100 °C for 24 hours to yield a fibrous, purple solid. The intrinsic viscosity of the polymer, measured in methanesulfonic acid (MSA) at 30 °C using a Cannon Ubbelohde viscometer, was 26.4 dl/g.

Synthesis of Poly(benzobenzobisoxazole) containing naphthalene-1,5-diyl unit (Naph-1,5-PBO)

Into a resin flask fitted with a high torque mechanical stirrer, a nitrogen inlet/outlet adapter and a side opening for addition, was placed 4.32 g (0.02 mole) of 1,5-naphthalenedicarboxylic acid, an equimolar amount of 4,6-diaminoresorcinoldihydrochloride (4.26 g) and 23.08 g of 77 % PPA. The contents of the flask were slowly warmed to 105 °C and the diaminedihydrochloride monomer was dehydrochlorinated over a period of 24 hours under a dry nitrogen flow. The mixture was cooled and 11.66 g of P_2O_5 was added to adjust the PPA composition to have 83 % P_2O_5 content and to ensure a final polymer concentration of 14 wt % in PPA. The mixture was maintained at 100 °C with stirring to ensure good homogeneity and the temperature was then raised to 165 °C and the polymerization was run overnight. Stir -opalescence characteristic of the anisotropic phase of the polymer in PPA, was observed. The polycondensation was continued at 180 °C for four hours and ~ 35 g of the viscous polymer dope was taken out for the fiber spinning process. The remaining dope was placed in large quantities of water and the fibrous polymer was chopped up in a Waring blender. The polymer was filtered off, soxhlet-extracted with hot water and finally dried *in vacuo* at 100 °C for 24 hours to yield a fibrous, dark yellow solid. The intrinsic viscosity of the polymer, measured in MSA at 30 °C, was 9.6 dl/g.

2-3. Fiber Processing

The polymeric fibers were spun from the lyotropic liquid crystalline phase of the polymer in PPA. Naph-2,6- and Naph-1,5-PBT fibers were fabricated by a dry-jet wet spinning method using a custom-made device. The polymer dope was deaerated at 100°C and filtered through a 74 μm stainless steel mesh. The polymer fibers were then spun at 90°C with draw ratios in the range of 35-45. Subsequently, the fibers were soaked in large amounts of distilled water for several days to remove the residual acid. The air-dried fibers were then heat-treated in dry nitrogen at elevated temperatures (550ºC) for structure development (X-ray diffraction).

2-4. General Characterization

Optical microscopy on the polymer dope was performed using a Leitz polarizing microscope. Thermogravimetric analyses of the bulk polymer samples were performed both in helium and air using TA Instruments TGA 2950 Analyzer at a heating rate of 10 °C/min. For tensile testing, Naph-2,6-PBO and Naph-1,5-PBO fibers were annealed at 350 °C under a nitrogen atmosphere for 10 min. The tensile

modulus and the strength were determined using an Instron Universal testing machine at a strain rate of 1 %/min.

2-5 X-ray Studies

Wide-angle X-ray diffraction patterns were recorded on a phosphor image plate (Molecular Dynamics©) in a Statton camera. Monochromatic CuK_{α} radiation from a rotating anode X-ray generator operating at 40KV and 240 mA was used. The sample to film distance was calibrated by SiO_2 powders. The total intensity of each reflection was measured by using FIT2D software.[26] The intensity of a reflection having a maximum at 2θ (Bragg angle) and ζ (azimuthal angle) was integrated along the azimuthal direction from ζ_1 and ζ_2 at each 2θ ranging from $2\theta_1$ to $2\theta_2$ ($2\theta_1<2\theta< 2\theta_2$ and $\zeta_1<\zeta<\zeta_2$; $2\theta_1$, $2\theta_2$, ζ_1, and ζ_2 were chosen to include the whole area of the reflection to integrate), and then the background was corrected and finally the peak area was integrated along the 2θ angle. Structure factor was calculated after multiplicity, Lorenz and Polarization correction.[27]

2-6. Molecular Modeling

Molecular modeling and simulation of the X-ray patterns were carried out using Cerius[2®] software. The conformational energy was calculated with *ab-initio* method using SPARTAN® program at the Hartree-Fock, 6-31G** level while the energy in the crystal was calculated from the discover module of Cerius[2®] with force field of cvff (consistent valence force field).[28] Figure 1 shows the chemical structures of Naph-2,6-PBO and Naph-1,5-PBO along with the numberings of the atoms where torsion angle ϕ and rotational angle φ are defined. The bond angle and bond length were constrained with the values used in the model of PBO.[17] The rotational angle φ in the crystal structure was defined as the angle between the *ac* plane and the naphthalene ring on the projected *ab* plane. The conformational energies of benzobisoxazolenaphthalene-2,6-diyl and benzobisoxazolenaphthalene-1,5-diyl units were calculated at $10°$ increment of the torsion angle ϕ. The oxygen atoms in the benzobisoxazole ring are on the same side in the polymer repeat unit, i.e., they have the *cis*-PBO configuration derived from the polycondensation of naphthalene-2,6- or 1,5-dicarboxylic acids with 4,6-diaminoresorcinoldihydrochloride.

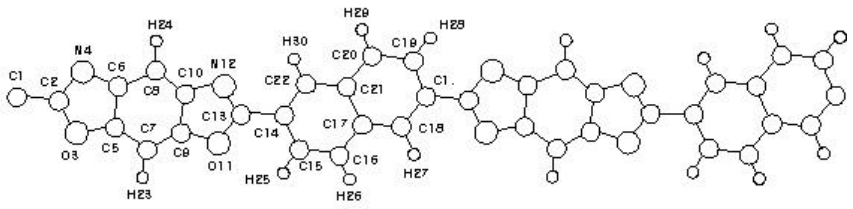

(a)

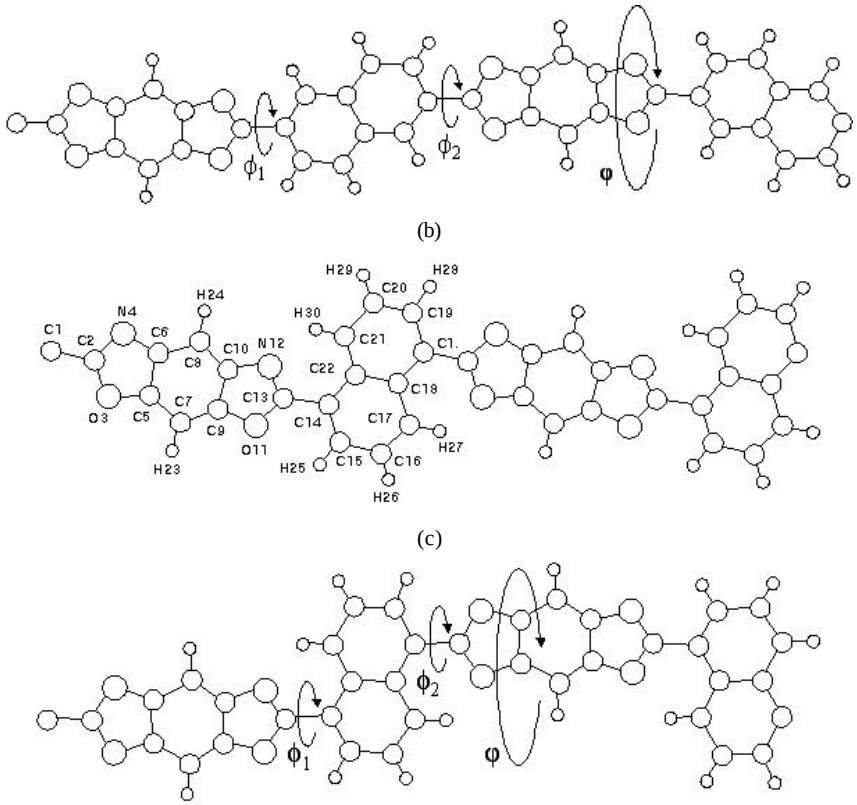

Figure 1. The chemical structures of Naph-2,6-PBO and Naph-1,5-PBO where torsion angle ϕ and rotational angle φ were defined; the (a) *trans* and (b) *cis* chain conformations of Naph-2,6-PBO and the (c) *trans* and (d) *cis* chain conformations of Naph-1,5-PBO; the torsion angle ϕ is O_{11}-C_{13}-C_{14}-C_{15} and rotation angle φ is 0° when the naphthalene ring is parallel to the *ac* plane in the crystal and the clockwise direction is +.

2-7. Refinement

The structural refinement was performed by using winLALS software [29,30] with the constrained least-square method in which the bond lengths and bond angles reported by Fratini *at al.*[17] were used. The parameters to be refined are the Eulerian angles which are convertible to the rotation angle φ, torsion angle between the benzobisoxazole and naphthalene ring ϕ, the isotropic temperature factor B_{iso} and the scale factor.

3. Results and discussion

3-1. Polymer synthesis and characterization

The reaction scheme for the formation of Naph-2,6-PBO and Naph-1,5-PBO is shown below (Figure 2).

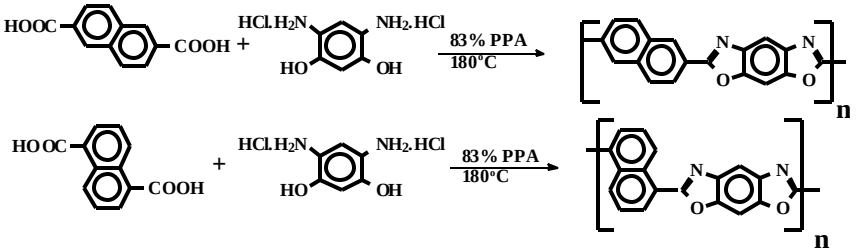

Figure 2. Synthesis of poly(benzobisoxazole)s with naphthalene-2,6-diyl and naphthalene-1,5-diyl structural units

Evidence for the presence of the lyotropic mesophase of the rigid-rod polymer in PPA was obtained by the observation of optical birefringence of a sample of the dope sealed between glass slides and examined under polarizing optical microscopy (POM) (Figure 3). The example shown here is that of 12 wt % Naph-2,6-PBO in PPA.

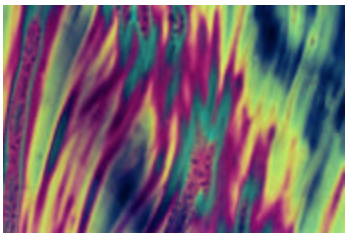

Figure 3. Polarizing optical micrograph of 12 wt % Naph-2,6-PBO in PPA

The polymers were of high molecular weight, as evidenced by the measured intrinsic viscosities of the two dilute polymer solutions in the strong acid solvent MSA and the fact that they could be continuously spun into fibers at relatively high draw ratios using a dry-jet wet spinning method. The thermal and thermooxidative stabilities were also high, as evidenced by the TGA analyses of both bulk polymers, shown in Figure 4. The onset of thermal degradation in helium and in air occurred at 650°C and 580°C for Naph-2,6-PBO. The poly(benzobisoxazole) with the naphthalene-1,5-diyl unit exhibited a somewhat lower stability, the onset of thermal degradation being 600°C and 550°C in helium and in air, respectively.

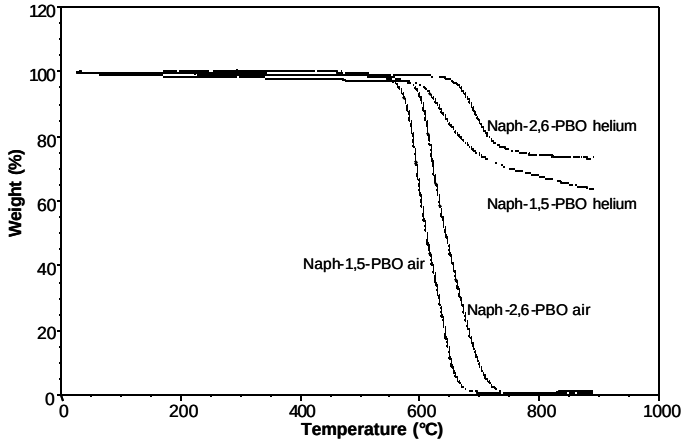

Figure 4. TGA of Naph-2,6-PBO and Naph-1,5-PBO in helium and in air

The measured mechanical properties indicated a tensile modulus of 60 GPa and a tensile strength of 2.5 GPa for the annealed Naph-2,6-PBO fibers. Annealed Naph-1,5-PBO fibers exhibited a tensile modulus of 32.5 GPa and a tensile strength of 1.2 GPa. In the case of both, heat treatment resulted in a perceptible enhancement in the tensile modulus relative to the as-spun fibers. The elongation at break decreased to 3.8 % upon heat-treatment from 6.4 % for the as-spun Naph-2,6-PBO fibers; a similar decrease was observed for Naph-1,5-PBO fibers (3.7 % for the heat treated fibers vs 8 % for the as-spun fibers). The lower fiber tensile properties of Naph-1,5-PBO relative to its Naph-2,6-PBO counterpart can be attributed to the more pronounced kinks in the chain conformation of Naph-1,5-PBO (*vide infra* for a discussion on the structural aspects).

3-2. X-ray patterns

Figures 5a and 5c show the X-ray fiber patterns of Naph-2,6-PBO and Naph-1,5-PBO before annealing, respectively. Two broad, strong equatorial reflections and several ordered meridional reflections were observed for both Naph-2,6-PBO and Naph-1,5-PBO fibers. These patterns are typical of X-ray fiber patterns of rigid-rod polymers. The *d*-spacings of the first equatorial reflections are 6.01 Å and 6.88Å for Naph-2,6-PBO and Naph-1,5-PBO, respectively which are larger compared to that of PBO (5.8Å)[17]. The *d*-spacings of the second equatorial reflections are 3.40 Å and 3.50Å respectively for Naph-2,6-PBO and Naph-1,5-PBO, which are similar to that of PBO (~3.5Å).[17] The first and second reflections represent the side-by-side and the face-to-face packing in the crystal, respectively. The spacing of the side-by-side packing for both Naph-2,6-PBO and Naph-1,5-PBO increases compared to

that of PBO due to the large naphthalene ring although the spacing due to the face-to-face packing is not much affected by the incorporation of the naphthalene unit. The fiber repeat distances are 14.15Å and 12.45Å for Naph-2,6-PBO and Naph-1,5-PBO, respectively, which are larger than that of PBO (12.0Å)[17]. The longer fiber repeat distance for Naph-2,6-PBO is due to the more linear shape along the chain axis. The more kinked structure of Naph-1,5-PBO seems to be reflected on the larger spacing of the side-by-side packing and the shorter fiber repeat distance (relative to Naph-2,6-PBO) in the crystal.

Figures 5b and 5d show the X-ray fiber patterns of Naph-2,6-PBO and Naph-1,5-PBO after annealing. The evolution of the three-dimensional order upon annealing is evident from the appearance of the new reflections. However, the axial disorder is still present, which can be inferred from the streaks along the layer lines. Naph-2,6-PBO has more profound streaks along the layer lines than Naph-1,5-PBO. The axial disorder is known to be due to the linear shape of the rigid-rod polymer chain. Naph-2,6-PBO may have more axial disorder than Naph-1,5-PBO because Naph-2,6-PBO has a more linear shape than Naph-1,5-PBO. The two equatorial reflections become sharper for Naph-1,5-PBO and are separated into three reflections for Naph-2,6-PBO indicating that crystal size and regularity in the crystal increase and the disorder decreases during annealing. A streak on the first layer line and two distinct reflections on the second layer line were observed for both Naph-2,6-PBO and Naph-1,5-PBO. There is a distinct meridional reflection on the fourth layer and several diffuse reflections on the higher layer lines for Naph-2,6-PBO.

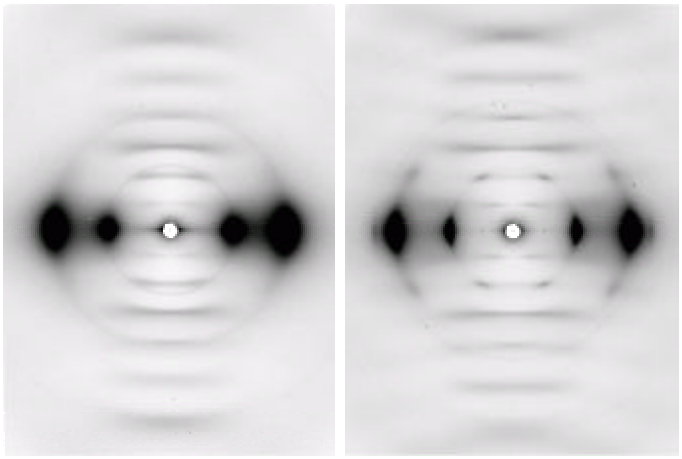

(a) (b)

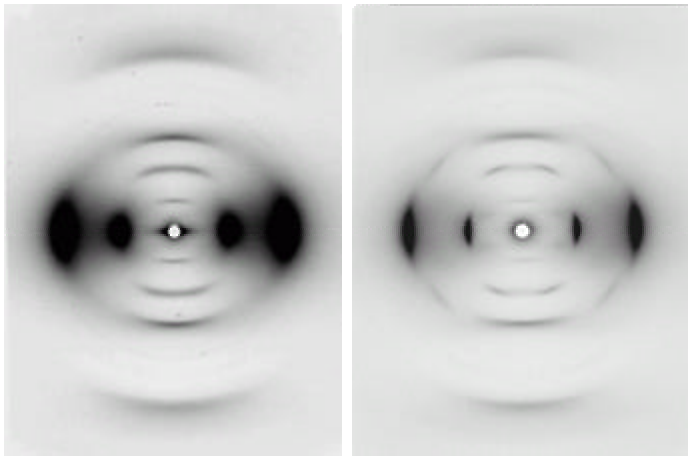

(c) (d)

Figure 5. X-ray fiber patterns of Naph-2,6-PBO and Naph-1,5-PBO before and after annealing: Naph-2,6-PBO (a) before and (b) after annealing; Naph-1,5-PBO (c) before and (d) after annealing.

3-3 Chain Conformation

Figure 1 shows the two possible conformations (*trans* and *cis*) of Naph-2,6-PBO and Naph-1,5-PBO; here, *cis* and *trans*, refer to chain conformation, and represent different terminologies from those of *cis*-PBO and *trans*-PBO, which stand for configuration. The *trans* conformation can consist of the one monomeric unit, whereas the *cis* conformation consists of two monomeric units at least. The fiber repeat distances are identical to the length of one repeat unit indicating that both Naph-2,6-PBO and Naph-1,5-PBO may adopt the *trans* conformation although detailed chain conformation should be studied with X-ray results. Two torsion angles (ϕ_1 and ϕ_2) for the *trans* conformation are in different environments although those for the *cis* conformation are in the same environment as shown in Figure 1. The conformation at ϕ_1=0° is when the naphthalene ring is rotated toward nitrogen and the conformation at ϕ_1=180° is when the naphthalene ring is rotated toward oxygen. The coplanar structure is when (ϕ_1, ϕ_2) is (0°, 180°) (or (180°,0°)) for the *trans* conformation and (ϕ_1, ϕ_2) is (0°, 0°) (or (180°, 180°)) for the *cis* conformation.

Figure 6 shows the *ab-initio* conformational energy of PBO, Naph-1,5-PBO, and Naph-2,6-PBO with respect to the torsion angle, ϕ. The conformational energy of PBO is essentially the same as that reported earlier showing the symmetric curve with the maximum at ϕ=90° although those of Naph-2,6-PBO and Naph-1,5-PBO are not symmetric due to the fused naphthalene ring (formation of kinked structures). The energy barrier to the perpendicular conformation (ϕ=90°) of PBO is 2.3 kcal/mole, which is very close to the reported value of 2.52 kcal/mole.[31] In the case of Naph-2,6-PBO, the energy is minimum at ϕ=180° with the local minimum at ϕ=0°. The energy difference between ϕ=180° and 0° is only ~0.3 kcal/mole while the energy barrier to the perpendicular conformation becomes ~7.8kcal/mole,

which is large compared to that of PBO (2.3 kcal/mole). The conformational energy of Naph-2,6-PBO suggests that Naph-2,6-PBO is stable in the planar structure at ϕ_1=0° and ϕ_2=180°. In the case of Naph-1,5-PBO, the energy is minimum at ϕ=180° with the local minimum at ϕ=~25°. However, the energy is quite flat from ϕ=-30° to ϕ=30°; the gap between the maximum and minimum energies in this region is only ~0.2 kcal/mole, suggesting that the torsion angle in the crystal can have a wide distribution in this region although inter-chain interaction in the crystal can change the torsion angle. More than two repeat units are needed for the chain structure to be linear if the chains are in the energetically stable conformation. However, if the torsion angles, ϕ_1 and ϕ_2 were the same with different signs, the fiber repeat distance would be the length of one monomeric unit. The detailed structure will be discussed later.

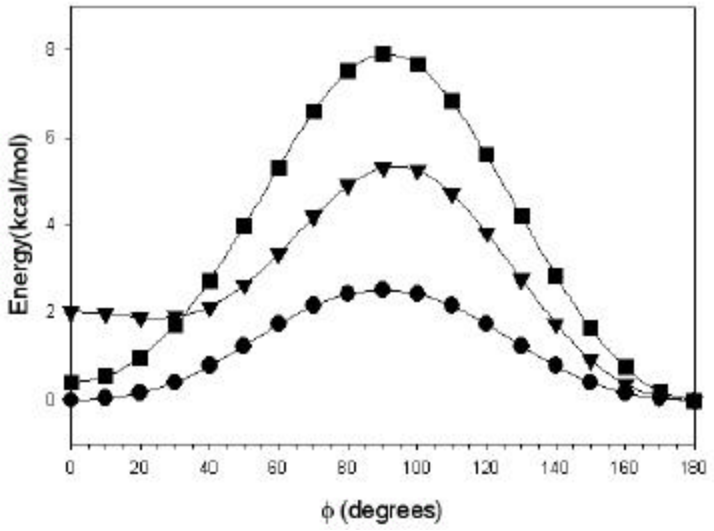

Figure 6. The *ab-initio* conformational energy of PBO (?), Naph-1,5-PBO (?) and Naph-2,6-PBO (¦) with respect to the torsion angle, ϕ.

3-4. The crystal structure

3-4-1. Naph-2,6-PBO

Figure 5b shows the X-ray fiber pattern of annealed Naph-2,6-PBO. The first and second strong equatorial reflections of Naph-2,6-PBO at *d*=6.01 Å and *d*=3.40 Å can be indexed as *100* and *010*, respectively (a^*=1/6.01 Å^{-1} and b^*=1/3.40 Å^{-1}). The *d*-spacing of the third weak equatorial reflection is *d*=2.99 Å which is half of the *d*-spacing of the first equatorial reflection and can be indexed as *200*. The g^* value cannot be determined from the equatorial reflections due to the limitation of the number of the independent reflections. The *d*-spacing of the *110* reflection is 2.97 Å with the assumption of g^*= 90° so

that the reflection at d=2.99 Å can be overlapped with *200* and *110* reflections (the g^* will be discussed later). Two distinct reflections on the second layer line at d=6.11 Å and 3.45 Å indicate that there is a registry between the adjacent chains in the crystal system like other rigid-rod polymers such as PBO and PBT. The Radius values of the cylindrical coordinates of the first and second reflections on the second layer line in the reciprocal space are 0.083 $Å^{-1}$ and 0.253 $Å^{-1}$, respectively. The Radius value of the first reflection on the second layer line (0.083 $Å^{-1}$) is half of the Radius value of the first equatorial reflection ($1/d_{100}$=0.167 $Å^{-1}$). The difference of the Radius value between the first and second reflections on the second layer line is 0.17 $Å^{-1}$ which is the same as the Radius value of the first equatorial reflection ($1/d_{100}$= ~0.17 $Å^{-1}$). Thus, the first and second reflections on the second layer line can be indexed as *002* and *102* (or *-102*), respectively. The angle between a^* and c^*, b^* is 59.7° and the staggering ratio ($\Delta c/c$) between adjacent chains in the *ac* plane of the crystal structure is 0.25. The a^* can be reduced to half of the original value by indexing the first equatorial reflection as *200* (the *a* dimension in real space will be doubled). Two reflections on the second layer line can be *002* and *202* reflections like PBO and PBT, as studied by Fratini *et al*[17] by using the large unit cell. In this unit cell, the second chain is in the middle of the *ac* plane of the orthorhombic cell with the axial shift of 0.3*c* against the corner chains for PBO. Thus, the sequence of the axial shift in the *ac* plane is an alternating +0.3*c* and -0.3*c*. However, it is quite difficult for the kinked structure to be packed into the large orthorhombic cell because one half of the chain along the chain axis has a completely different environment from the other half of the chain due to the kinked structure so that there is the possibility that chains are staggered in the same direction, i.e., all + (or all -) directions.

The two dimensional monoclinic unit cells were constructed with keeping a^* and b^* values and changing the g^* value. The g^* value for Naph-2,6-PBO was determined from the refinement of *hk0* reflections by finding the minimum R value for different unit cells. The projection along the *c* axis in the crystal is not affected by the axial disorder. The equatorial *hk0* reflections represent the projected structure along the *c* axis. The equatorial *hk0* reflections of the crystal are affected by the torsion and rotation angles because there is one chain in the unit cell. The final parameters are obtained by the constrained LALS method. During the refinement, the torsion angles were fixed as ϕ_1=0° and ϕ_2=180° for the minimum energy conformation, and the rotation angle was refined. The minimum R value was found at g^*=74º, which is similar to that of PBO (78.7°). The rotation angle φ was -8.6°. Regarding the small B_{iso}, 0.12 may be attributed to the rigidity of the molecules.

Figure 7 shows the calculated energy of the crystal with respect to the staggering ratio ($\Delta c/c$) in the *ac* plane while keeping the same *ab* projection of the crystal structure. The unit cell was calculated by changing b^* while keeping the other reciprocal lattice parameters constant. The calculated unit cells have the same *ab* projection in the real space and the staggering ratio can be controlled by b^*. The minimum energy was found at $\Delta c/c$=-0.25. The value of $\Delta c/c$=-0.25 was close to the value studied by X-ray. The energy at $\Delta c/c$=0.25 is quite high compared to that at $\Delta c/c$=-0.25. In order to have two reflections on the second layer, the possible $\Delta c/c$'s are +0.25, -0.25, and ±0.25 (+ and – signs are random). However, the

$\Delta c/c$'s of +0.25 and ±0.25 are improbable in the crystal structure due to the high energy at $\Delta c/c$=+0.25 suggesting that the occurrence of the random structure is difficult in the *ac* plane of the crystal. Figure 8 shows the calculated energy of the crystal *versus* the staggering ratio ($\Delta c/c$) in the *bc* plane while keeping the same *ab* projection of the crystal structure and staggering ratio of 0.25 in the *ac* plane. Several energy minima at $\Delta c/c$=±0.06, ±0.25, and ±0.4 were found, suggesting that the disorder structure is due to random staggering in the *bc* plane rather than in the *ac* plane.

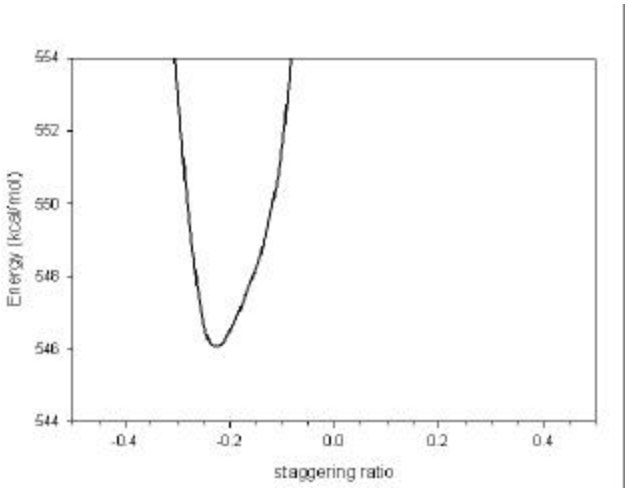

Figure 7. The calculated energy of the crystal with respect to the staggering ratio ($\Delta c/c$) in the *ac* plane while keeping the same *ab* projection of the crystal structure.

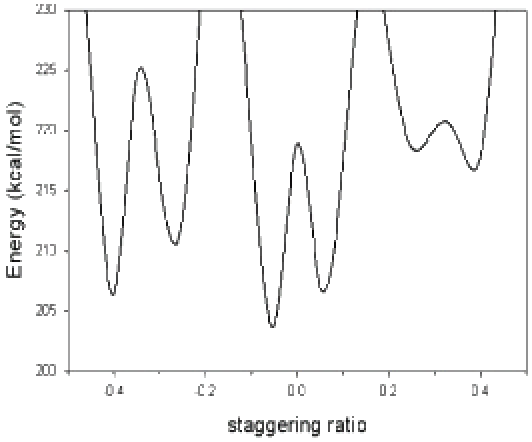

Figure 8. The calculated energy of the crystal *versus* the staggering ratio ($\Delta c/c$) in the *bc* plane while keeping the same *ab* projection of the crystal structure and staggering ratio of 0.25 in the *ac* plane.

We could not define the unit cell parameters because of the undetermined α^* value. However, the projection along the chain axis and the ac projection can be drawn from the X-ray results as shown in Figure 9. In the *ac* projection (Figure 9a), the kinked chains of Naph-2,6-PBO are staggered side-by-side by 0.25*c*. The 0.25*c* staggering between the adjacent chains provides optimum packing in the crystal without any steric interaction. In the projection along *c* axis (Figure 9b), the chains are packed closely and the naphthalene rings are rotated by 8.6(±2)° from the *ac* plane.

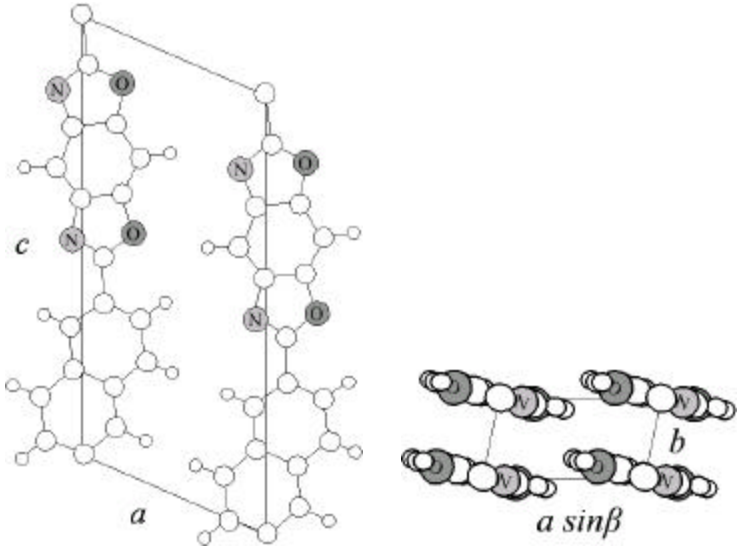

(a) (b)

Figure 9. The (a) *ac* projection, and (b) the projection along the chain axis of the crystal structure of Naph-2,6-PBO.

3-4-2. Naph-1,5-PBO

Figure 5d shows the X-ray fiber pattern of annealed Naph-1,5-PBO. The X-ray fiber pattern of Naph-1,5-PBO is different from that of Naph-2,6-PBO in terms of the streaks along the layer lines. The steaks in the X-ray fiber pattern are not profound compared to those of Naph-2,6-PBO. Short streaks at the meridian on the first and second layer lines are observed indicating that the axial disorder still exists although it is not severe compared to that of Naph-2,6-PBO. The X-ray fiber pattern suggests that Naph-1,5-PBO is closer to the perfect three dimensional crystal with a small degree of the axial disorder. The first and second strong equatorial reflections at d=6.88 Å and d=3.50 Å can be indexed as *100* and *010*, respectively (a^*=1/6.88 Å^{-1} and b^*=1/3.50 Å^{-1}). The *200* reflection (d_{200}=3.44 Å) observed for Naph-1,5-PBO overlaps with the *010* reflection (d_{010}=3.50 Å) due to their close d-spacings. The g^* value can't be

determined from the equatorial reflections for the same reasons as in the case of Naph-2,6-PBO. The Radius values of the cylindrical coordinates of the first and second reflections (d=5.75Å and 3.70Å) on the second layer line in the reciprocal space are 0.065 $Å^{-1}$ and 0.217 $Å^{-1}$, respectively. The difference of the Radius value between the first and second reflections on the second layer line is 0.152 $Å^{-1}$ which is the same as the Radius value of the first equatorial reflection ($1/d_{100}$= ~0.15 $Å^{-1}$). Thus, the first and second reflections on the second layer line can be indexed as *002* and *102* (or *-102*), respectively. The angle between a^* and c^*, b^* is 67.2° and the staggering ratio ($\Delta c/c$) is 0.23, which is a little smaller than that of Naph-2,6-PBO (0.25). In order for the repeat unit to be a monomeric unit, the torsion angles, ϕ_1 and ϕ_2 should be the same value with different signs as mentioned before. The torsion angles of ϕ_1 and ϕ_2 can be 25° and -25°, respectively with a little energy cost at ϕ_1. We can predict a fiber repeat distance of 12.45Å, which is coincident with X-ray results in these torsion angles. The g^* value of 76° and the rotation angle of 18.4° were refined from the same method for Naph-2,6-PBO with the torsion angles of ϕ_1=25° and ϕ_2=-25°. We could not define the unit cell parameters because of the same reason as for Naph-2,6-PBO i.e. the undetermined α^* value. Figure 10 shows the ac projection and the projection along the chain axis of the crystal structure. In the projection along the chain axis (Figure 10b), the chains are close packed and the naphthalene rings are rotated by 18.4° from the *ac* plane. In the ac projection (Figure 10a), the kinked chains of Naph-1,5-PBO are staggered side-by-side by 0.23c. The 0.23c staggering between the adjacent chains gives perfect packing in the crystal without any steric interaction. Naph-1,5-PBO has the kinked structure which is attributable to the naphthalene unit, as well as the twisted structure which is caused by the torsion angle. The kinked and twisted chain structure of the rigid-rod chain in the crystal seems to prevent slippage between the adjacent chains in the crystal structure. The more perfect crystal structure of Naph-1,5-PBO may be due to this difficulty in the occurrence of the slippage.

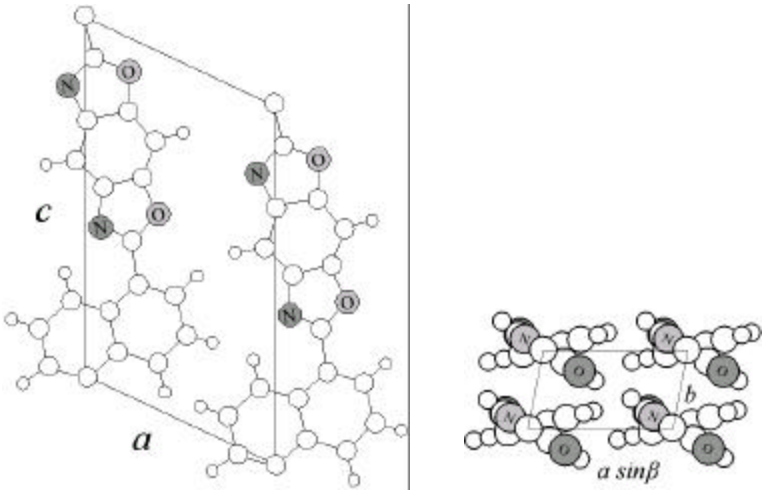

(a) (b)

Figure 10. The (a) *ac* projection and (b) the projection along the chain axis of the crystal structure of Naph-1,5-PBO.

4. Conclusions

The crystal structure of Naph-2,6-PBO and Naph-1,5-PBO are different from PBO due to the kinked chain structure introduced by the 1,5- and 2,6- positions at which the naphthalene ring is extended. The main difference between Naph-1,5-PBO and Naph-2,6-PBO is that Naph-1,5-PBO has a more kinked and congested structure than Naph-2,6-PBO because the distance between the hetero atom of the heterocyclic ring and the alpha hydrogen of the naphthalene ring of Naph-1,5-PBO is close enough to cause steric interaction with each other.

We found, that in general, the X-ray fiber pattern of Naph-2,6-PBO is similar to that of PBO in terms of reflections on the equator as well as the streaks along the higher layer lines. From the X-ray fiber patterns, we found that the spacing of the side-by-side packing increases due to the large naphthalene unit although the spacing due to the face-to-face chain packing is not much affected by the incorporation of the naphthalene unit. The repeat unit distance for Naph-2,6-PBO (14.15 Å) was found to be larger compared to that of PBO (12.0 Å) due to the fused aromatic ring system of the naphthalene unit. The X-ray fiber pattern of Naph-2,6-PBO suggests that the registry between adjacent chains exists in the crystal with a lot of axial disorder. The extent of staggering between the adjacent chains is 0.25*c*. From the refinement method, the projected crystal structure is proposed. In this model, the naphthalene ring is rotated by 8.6° from the *ac* plane on the project ion along the chain axis with the torsion angle between the naphthalene and heterocyclic rings of ~0°.

Naph-1,5-PBO has a kinked structure due to the 1,5- positions of the naphthalene ring at which the heterocyclic rings are extended as well as the twisted structure due to steric hindrance between the hetero atom in the heterocyclic ring and α-hydrogen in the naphthalene ring. These structural differences change not only the chain conformation but also the crystal structure, especially the disorder in the crystal. The torsion angle between the heterocyclic and naphthalene rings, ϕ is ~25°, which was derived from the *ab-initio* energy calculation as well as the crystal structure refinement. We found from the crystal model that the zig-zagged structure is well packed side-by-side in the *ac* plane. The naphthalene ring is rotated by 18.4° from the *ac* plane and the chains are staggered side-by-side by 0.23*c* in a regular way in the ac plane. The kinked and twisted structure of the rigid-rod chain in the crystal seems to prevent slippage between the adjacent chains in the crystal structure.

5. References

(1) Ulrich, D.R. *Polymer* 1987, 28,533

(2) Roche, E.J.; Takahashi, T.; Thomas, E.L. *ACS Symp. Ser.* 1980, 141, 303

(3) Odell, J.A.; Keller, A.; Atkins, E.D.T.; Miles, M.J. *J. Mater. Sci.* 1981, 116, 3309

(4) Adams, W.W.; Eby, R.K. *MRS Bull.* 1987, 12, 22

(5) Allen, S.R.; Filippov, A.G.; Farris, R.J.; Thomas, E.L.; Wong, C.P.; Berry, G.C.; Chenevey, E.C. *Macromolecules* 1981, 14,1135

(6) Wolfe, J.F.; Arnold, F.E. *Macromolecules* 1981, 14, 909

(7) Wolfe, J.F.; Loo, B.H.; Arnold, F.E. *Macromolecules* 1981, 14, 915

(8) Choe, E.W.; Kim, S.N. *Macromolecules* 1981, 14, 920

(9) Cotts, D.B.; Berry, G.C. *Macromolecules* 1981, 14, 930

(10) Welsh, W.J.; Bhaumik, D.; Mark, J.E. *Macromolecules* 1981, 14, 947

(11) Welsh, W.J.; Bhaumik, D.; Jaffee, H.H.; Mark, J.E. *Polym. Eng. Sci*. 1984, 24, 218

(12) Welsh, W.J.; Mark, J.E. *J. Mater. Sci*. 1983, 18, 1119

(13) Bhaumik, D.; Welsh, W.J.; Jaffee, H.H.; Mark, J.E. *Macromolecules* 1981, 14, 951

(14) Wellman, M.W.; Adams, W.W.; Wolff, R.A.; Dudis, D.S.; Wiff, D.R.; Fratini, A.V. *Macromolecules* 1981, 14, 935

(15) So, Y. H. *Prog. Polym. Sci.* 2000, 25, 137

(16) Wierschke, S.G. Master Thesis, Wright State University, Ohio, 1988

(17) Fratini, A.V.; Lenhert, P.G.; Resch, T.J.; Adams, W.W. *Mater. Res. Soc. Symp. Proc.* 1989, *134*, 431

(18) Martin, D.C.; Thomas, E.L. *Macromolecules* 1991, *24*, 2450

(19) Tashiro, K.; Yoshino, J.; Kitagawa, T.; Murase, H.; Yabuki, K. *Macromolecules* 1998, *31*, 5430

(20) Takahashi, Y. *Macromolecules* 1999, *32*, 4010

(21) Tonelli, A.E. *Polymer*, 2002, 43, 637

(22) Matsuoka, T.; Kubota, F. *Jpn. Kokai. Tokkyo. Koho* 1998, JP 10158213 (assigned to Toyobo Co., Ltd., Japan)

(23) Dang, T.D.; Venkatasubramanian N.; Talicska, A.; Park, S.-Y.; Arnold, F.E. *Polymer Preprints (American Chemical Society)* 2002, 43(1), 660

(24) Park, S.-Y.; Moon, S-C.; Dang, T. D.; Venkatasubramanian, N.; Lee, J-W.; Farmer, B. L. *Macromolecules* (Accepted), 2005

(25) Wolfe, J. F. *Encyclopedia of Polymer Science and Engineering*, 1988, 11, 601

(26) www.esrf.fr/computing/scientific/FIT2D/

(27) Okuyama, K.; Noguchi, K.; Miyazawa, T.; Yui, T.; Ogawa, K. *Macromolecules* 1997, 30(19), 5849

(28) www.accelrys.com/doc/life/cerius46/

(29) Arnott, S.; Wonacott, S. *Polymer* 1966, 7, 157

(30) Smith, P.J.C.; Arnott, S. *Acta Crystallogr. Sect. A* 1978, 34, 3

(31) Farmer, B.L.; Wierschke, Scott G.; Adams W.W. *Polymer* 1990, 31, 1637

6. PI's *Curriculum Vitae*

Education:

1995 ~ 1998	**Ph.D**., Department of Macromolecular Science **Case Western Reserve University** Title: "The Crystal Structure and Molecular Modeling of Three Novel Polymers" Advisor: Professor John Blackwell
1988~1990	**M.S**., Department of Fiber and Polymer Science **Seoul National University**, Seoul, Korea Title: "Piezoelectricity and Curie Transition of Blends of P(VDF-co-TrFE) and PMMA" Advisor: Professor Sang-Yong Kim
1984~1988	**B.S**., Department of Textile Engineering **Seoul National University**, Seoul, Korea

Experiences:

2002 ~ present	**Kyungpook National University, Department of Polymer Science**
1998 ~ 2002	**National Research Council Research Associate at Air Force Research Laboratory/Polymer Branch**
1990 ~1995	Senior Researcher, R&D Center, Cheil Synthetics Inc., **Samsung**, Gihung, GyungKi, Korea

Affiliations

American Chemical Society,
American Physical Society
American Crystallographic Association
Korean Polymer Society
Korean Textile SocietyAffiliations

7. Publications:

2005.

1. Soo-Young Park, Yang-Hwan Cho, Richard A. Vaia, “Three-dimensional structure of the zone-drawn film of the nylon-6/layered silicate nanocomposites”, *Macromolecules*, 38(5), 1729 (2005).

2. Soo-Young Park, Sang-Cheol Moon, Thuy D. Dang, N. Venkatasubramanian, Jar-wha Lee and B.L. Farmer, "Crystal structure of poly(1,5-naphthalenebenzobisthiazole)", *Macromolecules*, 38(5), 1711 (2005).

3. Jong-Beom Baek, Soo-Young Park, Gary E. Price, Christopher B. Lyonsd, and Loon-Seng Tan, "Unusual thermal relaxation of viscosity-and-shear-induced strain in poly(ether-ketones) synthesized in highly viscous polyphosphoric acid/P2O5 medium",
Polymer, 46, 1543-1552 (2005).

4. Soo-Young Park, Seung-Woo Lee, Tae-Jin Oh, and John Blackwell, "Crystal Structure of Poly(2-cyano-1,4-phenylene terephthalamide)", Macromolecules, 38, 3713 -3718 (2005).

5. Soo-Young Park and Yang-Hwan Cho, "Thermal Transitions of the Drawn Film of a Nylon 6/Layered Silicate Nanocomposite", Macromolecular Research, 13(2), 156-161 (2005)

6. Soo-Young Park, Sang-Cheol Moon, Thuy D. Dang, N. Venkatasubramanian, Jar-wha Lee and B.L. Farmer, "The Crystal structure of poly(2,6-naphthalenebenzobisthiazole)", Polymer, 46, 5630 (2005)

2004

1. Soo-Young Park, Hilmar Koerner, S. Putthanarat, Rahmi Ozisik, Shane Juhl, B. L. Farmer and R. K. Eby, "Structure of poly (p-phenylenebenzobisoxazole) (PBZO) and poly (p-phenylenebenzobisthiazole) (PBZT) for proton exchange membranes (PEMs) in fuel cells", Polymer, 45, 49 (2004)

2. Soo-Young Park, B.L. Farmer, and Jong-Chan Lee, "Effects of the Alkyl Side-Chain Length on the Structures of Poly[oxy(*N*-alkylsulfonylmethyl)ethylene]s", Journal of Polymer Science, Part B: Polymer Physics, 42(10), 1868-1874 (2004)

3. Lee Soon Park, Hyung Suk Choi, Woo-Sik Kim, Dong-Ho Lee, Kyung-Eun Min, Kwan-Ho Seo, Inn Kyu Kang, Soo-Young Park, Sung Ho Hwang, Younghwan Kwon,

"Photolithographic process of microcapsule sheet for electrophoretic display", Materials Science and Engineering C 24, 143-146 (2004)

4. Shin-Hee Lee, Soo-Young Park, Jae-Hong, "Choi Fiber formation and physical properties of chitosan fiber crosslinked by epichlorohydrin in a wet spinning system: the effect of the concentration of the crosslinking agent epichlorohydrin". Journal of Applied Polymer Science, 92(3), 2054-2062 (2004).

2003

1. Jong-Chan Lee, Se-Hui Hana, Sang-Ho Cha, Soo-Young Park, B.L. Farmer, "Synthesis and dipole-dipole interaction-induced mesomorphic behavior of poly(oxyethylene)s containing (n-octylsulfonyl)alkylthiomethyl or (n-octylsulfonyl) alkylsulfonylmethyl side groups", Polymer, 44, 7413 (2003)

2. Soo-Young Park, Leonard V. Interrante, B. L. Farmer, "Packing Studies on Poly(di-n-alkylsilylenemethylene)s", Macromol. Rapid Commun., 24, 793 (2003)

3. Tao Zhang, Soo-young Park, B. L. Farmer, L. V. Interrante, Synthesis of Comb-Type Polycarbosilanes via Nucleophilic Substitution reactions on the Main-Chain Silicon Atoms, "Journal of Polymer Science: Part A: Polymer Chemistry", 41, 984, (2003)

4. W.S. Kim, K.R. Byun, D.H. Lee, K.E. Min, L.S. Park, K.H. Seo, I.K. Kang, S.Y. Park, "Synthesis of photocrosslinkable polymers using abietic acid and their characterization", Polymer Journal, 35, 450 (2003)

5. H.W. Choi, Y.J. Jung, M.H. Lee, S.J. Lee, S.Y. Park, S.H. Lee, "Effects of Fineness of Chitosan Fiber on the Adsorption Characteristics of Metal Ion", J. of the Korean Soc. Of Dyers and Finishers, 15, 146 (2003)

6. Woo-Sik Kim, Min-Woo Kim, Eun-Chun Jung, Chang-Hoon Baek, Lee-Soon Park, Inn-Kyu Kang, Soo-Young Park, "Synthesis and characterization of polyacrylate derivatives having protected isocyanate groups and fluorinated alkyl groups", Polymer (Korea), 27, 364 (2003)

7. Ho-Gyun Kim, Dong-Ho Lee, Kwan-Ho Seo, Soo-Young Park, Kyung-Eun Min, "Effect of organic modifiers and mixing times on the properties of unsaturated polyester/montmorillonite nanocomposite", Polymer(Korea), 27, 589 (2003)

8. Hae Wook Choi, Young-Jin Jung, Myung Hwan Lee, Soon Jang Lee, Soo Young Park, Shin Hee Lee, "Effects of fineness of chitosan fiber on the adsorption characteristics of metal ion", Journal of the Korean Society of Dyers and Fisheries, 15, 20 (2003)

2002

1. Cho, Kwang Soo; Kim, Woo Sik; Lee, Dong-Ho; Park, Lee Soon; Min, Kyung Eun; Seo, Kwan Ho; Kang, Inn-Kyu; Park, Soo-Young; Kwon, Youngdon. "A phenomenological

model for linear viscoelasticity of monodisperse linear polymers", Macromolecular Research, 10(5), 266-272,(2002),

2. Lee, J.-C.; Lim, M.-Y.; Oh, K.; Kim, Y. G.; Lee, H. B.; Park, S.-Y.; Farmer, B. L. "Synthesis and mesomorphic properties of poly(oxyethylene)s containing alkylsulfonylmethyl or alkylthiomethyl side groups". Polymer, 43(25), 7051-7061 (2002).

3. Park, S.-Y.; Zhang, T.; Interrante, L. V.; Farmer, B. L. "The structure of a cyanobiphenyl side chain liquid crystalline poly(silylenemethylene)". Polymer, 43(19), 5169-5174 (2002).

4. Park, Soo-Young, "Crystal structure analysis of polymeric materials using two-dimensional X-ray pattern and molecular modeling". Kobunja Kwahak Kwa Kisul , 13(2), 255-260 (2002).

5. Park, Soo-Young; Zhang, Tao; Interrante, L. V.; Farmer, B. L. "Structures of Side Chain Liquid Crystalline Poly(silylenemethylene)s". Macromolecules, 35(7), 2776-2783 (2002).

2001

1. Park, S.-Y.; Farmer, B. L.; Lee, J.-C. "The structures of poly(oxyethylene)s having sulfone groups in the side chains). Polymer, 43(1), 177-183 (2001).

2. Lee, Jong-Chan; Oh, Kyungseok; Lee, Hee Bong; Kim, Yong Gyu; Jho, Jae Young; Kwak, Seung-Yeop; Park, Soo-Young; Farmer, Barry L. "Synthesis and mesomorphic properties of poly(oxyethylene) with [(6-heptylsulfonyl)hexylthio]-methyl side groups". Macromolecular Rapid Communications, 22(11), 815-819 (2001).

3. Park, S.-Y.; Interrante, L. V.; Farmer, B. L. "The structures of poly(di-n-alkylsilylenemethylene)s". Polymer, 42(9), 4261-4269 (2001).

4. Park, S.-Y.; Interrante, L. V.; Farmer, B. L. "The structure of poly(di-n-propylsilylenemethylene)". Polymer, 42(9), 4253-4260, (2001).

2000

1. Park, S.-Y.; Blackwell, J.; Chvalun, S. N.; Nikolaev, A. A.; Mailyan, K. A.; Pebalk, A. V.; Kardash, I. E. "The structure of poly(cyano-p-xylylene)", Polymer, 41(8), 2937-2945 (2000).

1999

1. Park, Soo-Young; Blackwell, John; Chvalun, Sergei N.; Mailyan, Karen A.; Pebalk, Andei V.; Kardash, Igor E. " A Three-Dimensionally Oriented Texture for Poly(a,a,a',a'-tetrafluoro-p-xylylene). Macromolecules, 32(23), 7845-7852 (1999).

1997

3. Park, Soo-Young; Chvalun, S. N.; Blackwell, J. "Structure of a Ring-Containing Fluoropolymer". Macromolecules, 30(22), 6814-6818 (1997).

1996

1. Dae-Woo Ihm, Soo-Young Park, Cheol-Gyu Chang, Yoon-Sung Kim, Hwan-Kwang Lee, "Miscibility of Poly(ethy1ene terephthalate)/Poly(ethylene-2,6-naphthalate) Blends by Transesterification", Journal of Polymer Science: Part A: Polymer Chemistry, Vol. 34,284-2850 (1996)